*Research Article*

# Mechanical and Wear Studies on AA7075/Nano TiC/Graphite Hybrid Composites for Tribological Applications

**Clement Tom Scaria,[1] R. Pugazhenthi [ID],[1] Ajith Arul Daniel,[1] and K. Santhosh [ID][2]**

[1]*Department of Mechanical Engineering, Vels Institute of Science Technology and Advanced Studies, Chennai 600117, India*
[2]*Department of Mechatronics Engineering, Wollo University, Kombolcha Institute of Technology, Post Box No. 208, Kombolcha, Ethiopia*

Correspondence should be addressed to R. Pugazhenthi; pugal4@gmail.com and K. Santhosh; santhosh@kiot.edu.et

The current paper aims to study wear behaviour of AA7075 reinforced with different weight percentage of nano-TiC and graphite particles under dry sliding condition. TiC particles are taken in different weight percentages (5%, 10%, and 15%), and graphite was chosen as (3%, 4%, and 5%) along with three different levels of sliding speed, applied load, and sliding velocity. The fabrication was conducted using stir casting equipment, and the experiments were done using Taguchi's L27 orthogonal array. The Taguchi and ANOVA results applied load and percentage of TiC are the most influencing parameters which influences wear loss and friction coefficient

## 1. Introduction

Metal matrixes in unstructured foams and MMCs have the potential to be employed as steel and cast iron component substitutes, especially when matrix materials are light. Aluminium is the common material used in the manufacturing process. These composites have grown in popularity due to its overwhelmed corrosion resistance, enhanced strength, and reduced density. Over base alloys, it has better resistivity and rigidity [1–4]. In a wide range of applications, these composites are replacing traditional aluminium alloys. Recent advancements in aluminium-based composites have made them increasingly useful and important in the automobile and space industries. One of the most significant developments in composite studies is the inclusion of nanoreinforcement in aluminium alloys. One of the keys to success in nanocomposites is good strength even at low volume fraction [5, 6]. Composites are made utilising a variety of traditional techniques, including solid state and liquid state fabrication. Among the various fabrication techniques, ultrasonic stir casting was among the most advantageous methods for achieving good dimensional

precision and homogeneous dispersion of reinforcing particles to attain the final product [7]. Depending on the application, different types of reinforcing particles are employed to make the composites. Ceramic particles have a higher level of stability and rigidity, making them ideal for use as reinforcement particles in specific applications. The addition of hard cermet carbide particles to an aluminium alloy increases mechanical and tribological qualities as well as hardness at ambient and increased temperatures [8, 9]. There are various alternative techniques to improving composite characteristics. Lowering of matrix grain size and reinforcing particle size is among them. Traditional metal matrix composites are projected to have substantially superior microstructure stability and mechanical properties than nanocrystalline matrices enhanced by nanoreinforcements [10]. Mohan et al. investigated aluminium LM4-based composites reinforced with TaC ceramic powder, with reinforcements percentages ranging from 0.5 to 2 wt%. The materials were created using a powder metallurgy process. The dry sliding wear behaviour of the proposed composites was evaluated using a pin-on-disc apparatus, and the Taguchi design of experiment was adopted. It was also

discovered that the percentage of Ta/NbC (tantalum niobium carbide) reinforcement has an effect on the dry sliding wear rate. The results reveal that the use of hard ceramic composites in alloys has a significant impact on the dry slide wear resistance qualities [4]. Ramanaiah et al. conducted an experiment using Al7075 reinforced with TiC (2, 4, 6, 8, and 10) wt%, with a mean particle size of 2 m, using the stir casting method. It was also discovered that composites had a lower wear rate than alloys. With 8 wt% TiC, superior wear qualities and COF have been observed [11]. Priyaranjan Samal et al. conducted an experiment on AA5052 and TiC as matrix and reinforcing elements. When compared to the base material, the 9% TiC-reinforced MMCs showed a significant improvement, with a 32 percent rise in hardness, 78% increase in the tensile value. The COF values for the composites declined linearly as the TiC content and applied stress increased as a result of the formation of deep grooves with no plastic deformation at the 9% TiC-reinforced composites [12]. The composite is made by utilising a two-step stir casting method with volume fractions of silicon carbide and titanium carbide ranging from 5% to 15%. Dry sliding wear tests with a pin-on-disc wear tester were used to investigate the wear and frictional qualities. At room temperature without a lubricant, differing loads of 10N, 20N, and 30N were applied with varying sliding velocities (1 m/s, 2 m/s, and 3 m/s). TiC-reinforced composites had a microhardness rating that was 18.8% greater than SiC-reinforced composites. TiC had a wear rate of $2.1103 \, \text{mm}^3$/m, while SiC had a wear rate of $6.4103 \, \text{mm}^3$/m, according to the wear rate forecast. The wear rate increases as the load and sliding velocities increases [13, 14]. The friction and wear properties of the 15% SiC / 5% Gr/Al composites with various-size graphite additions were examined using squeeze casting technology. The friction coefficient of composites dropped after the addition of graphite, and wear resistance rose by 170 to 340 times [15]. The tribological behaviour of AMMCs reinforced with SiC and MoS2 in a variety of temperatures. The hybrid MMC were made using the compo casting method, which involved reinforcing different sizes of SiC (10, 20, 40 m) with 5059 aluminium alloy at various weight fractions (5, 10, and 15%), with the addition of MoS2 set at 2%. In addition to particle size and SiC weight percentage, process parameters such as load, sliding velocity, sliding distance, and temperature were evaluated, and the L27 orthogonal array was used to conduct the experiments. The best sliding condition was determined using the Taguchi and the ANOVA approach. When fine particles are reinforced at their maximum percentages, the wear rate is shown to be strong at 15% [16].

## 2. Experimental Details

*2.1. Materials Used.* The matrix material selected is an AA7075 with great ductility; tremendous strength, hardness, and good fatigue endurance are only a few of its remarkable mechanical properties. Due to microsegregation, it is more susceptible to embrittlement than several alloys[17]. The chemical composition of AA7075 is shown in Table 1. Titanium carbide (TiC) is chosen as a primary reinforcement

TABLE: 1: Composition for aluminium alloy 7075.

| Si | Fe | Cu | Mn | Mg | Zn | Ti | Cr | Al |
|------|------|-----|------|-----|-----|------|------|-----|
| 1.12 | 0.35 | 1.4 | 0.81 | 2.4 | 5.8 | 0.25 | 0.56 | Bal |

due to its good wear and corrosion resistance. Graphite is chosen as a secondary reinforcement because of its self-lubrication properties. The EDS image of AA7075 hybrid composites is shown in Figure 1.

*2.2. Experimental Set-Up.* AA7075 alloy is fabricated using the liquid casting method is used to create graphite and TIC composite. An electrical furnace with a graphite crucible is used to melting the base material AA7075. The process is kept at 850°C in temperature. The melted aluminium is mixed with the warmed graphite particles. Then, it is swirled at 500 rpm with the aid of an impeller connected to a speed control motor. Continue swirling until all of the particles are distributed equally [18]. In order to solidify, the charge is deposited into a temporary steel mould after being removed from the graphite crucible. The same procedure is repeated for AA7075/5% Gr is mixed with 5% and 10% of TiC. The casted composites have undergone T6 heat treatment. In order to improve the wettablity of matrix and reinforcement, magnesium is added to about 2% during the casting process. Test specimens are prepared as per the requirements of the testing methods. The process parameters and their levels are shown in Table 2.

*2.3. Dry Sliding Wear.* A pin-on-disc method was employed at various parameters, including applying force, sliding speed, and sliding distance, to assess the sliding wear behaviour of Al based hybrid composite. The tests were carried out in dry conditions in accordance with ASTM G9995 standards [19]. The test specimens, which had measurements of $10 \, \text{mm} \times 10 \, \text{mm} \times 30 \, \text{mm}$, were clamped against a spinning sharpened disc made of EN32 steel and hardened to RC60.

## 3. Result and Discussion

The experimental results for the input parameters are given in Table 3. Figure 2 shows the S/N ratio graph for wear loss. From the figure, it can be found that the load is the most influencing parameter for wear loss. When the load is minimum, the wear loss also decreases, and the wear loss is maintained between 15N and 30N. At 10N of applied load, the wear loss is very low. The weight percentage of TiC is the second most influencing parameter for wear loss. At the maximum percentage of TiC, the wear loss is deceased [20]. At 3%, the loss of particles in the composites is very low. At 15% of nano TiC and 3% of graphite, the hardness value of the developed composites is very high. In this case, the harder particles have high strength to with stand the wear loss. From this experiment, the optimum combination to attain maximum wear loss is 3% of graphite and 15% of TiC, 400 rpm of sliding distance, 10 N of applied load,
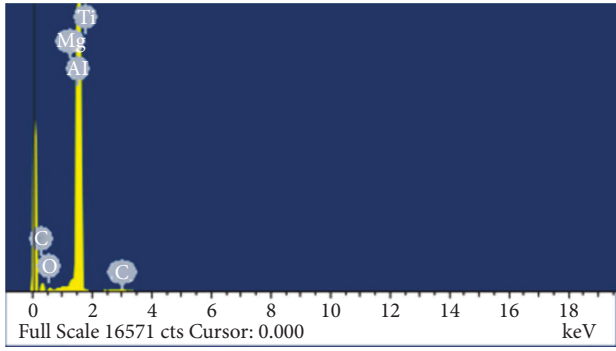
Figure 1: EDS image of AA7075 MMCs.

Table 2: Process parameters and their levels.

| Variable | Factor | Notation | Unit | Range | |
|---|---|---|---|---|---|
| | | | | Low | High |
| A | Titanium carbide | TiC | Wt. % | 5 | 15 |
| B | Graphite | Gr | Wt. % | 3 | 5 |
| B | Sliding speed | N | Rpm | 400 | 600 |
| D | Applied load | L | N | 10 | 20 |
| E | Sliding velocity | V | m/s | 0.5 | 1.5 |

and 0.5 m/sec of sliding velocity has minimum wear loss. The ANOVA table shows significant of wear loss in Table 4.

Figure 3 shows the coefficient of friction for the developed composites. The graph represents that the sliding velocity is the most affecting parameter which influencing the coefficient of friction. Increasing the sliding velocity increases the friction value. Next, the percentage of titanium carbide is the second influencing parameter for coefficient of friction. At 15% of TiC, the hardness of the developed composite is high, so that in that level, the friction is very low. When the applied load decreases, the coefficient of friction also decreases. At 10 N of applied load, the COF value is very low. At 400 rpm of sliding speed, the COF values decreases. This is due to the distance travelled between the pin and the disc ratio is very low so at that level the friction between the pin and the disc decreases [21]. The results shows that the optimum parameters to attain maximum coefficient of friction is 3% of graphite and 15% of TiC, 400 rpm of sliding distance, 10 N of applied load, and 0.5 m/sec of sliding velocity. Table 5 shows the ANOVA table significance for coefficient of friction.

Regression equation can be given as

$$\text{wear loss} = -0.000637593 + 0.000652222\,\text{Graphite}\,\% \\ -0.000114333\,\text{TiC}\,\% + 5.38333\text{e} \\ -006\,\text{Sliding Speed} + 7.26667\text{e} \\ -005\,\text{Load} + 0.00101222 \tag{1}$$

Sliding velocity can be given as

$$\text{COF} = 0.167846 + 0.00842222\,\text{Graphite}\,\% \\ -0.00411444\,\text{TiC}\,\% + 4.91111\text{e} \\ -005\text{Sliding Speed} + 0.00263889\,\text{Load} \\ + 0.0429778\,\text{Sliding Velocity} \tag{2}$$

Figure 4 shows the surface plot graph of titanium carbide and graphite weight percentage on wear loss during dry sliding wear behaviour. Increase in wt % of both reinforcement decreases the wear loss [22]. When the graphite percentage is 3% and 15%, then it increases the hardness of the composites. In that case, during dry sliding wear, the wear loss is very less.

Figure 5 shows the surface plot graph of sliding speed and load on wear loss. When the load and sliding speed increases, the wear loss in the composites increases. When the load is at 10 N, the wear loss is minimum; meanwhile, the wear loss increases at 15 N and sliding speed 500 rpm. In this work, the wear loss is suddenly low at 20N and the relation between sliding speed along and load along with material properties. The reading in that level during the experimentation the TiC 5% and Graphite is 5%, the hardness value is lower, and the wear loss is lower in this connection the wear loss was nearer to 15 N.

The relation between load and the sliding velocity is shown in Figure 6. The least domineering factor is for the wear loss. When the sliding velocity and load is higher and increases, the wear loss is higher in the developed composites. At 1.5 m/sec and when 20 N is the applied load, the wear loss is higher.

Figure 7 shows the surface plot for coefficient of friction between the weight percentage of titanium carbide and graphite. When the percentage of TiC increases, the COF increases. When the graphite percentage increases, the friction increases in a slow manner. The minimum influence on the graphite material is due to its self-lubrication properties and the friction between the pin and the disc decreases [23].

Figure 8 shows the interaction plot for coefficient of friction between load and sliding speed. When the load is at 10 N, the friction between the pin and the disc decreases; this is due to that the impact between the pin and the disc is low [24]. Meanwhile, when the load increases to 15N, the coefficient of friction increases. Meanwhile, when the load increases to 20%, the coefficient of friction slightly increases at that level. This is because of the presence of the graphite around 5% in this case, then the hardness of the composite material decreases due to the self-lubrant properties of graphite. Also, when the sliding distance of composites increase at 500 RPM, then the friction value also increases.

Figure 9 shows the interaction plot for coefficient of friction between load and sliding velocity. When the load and sliding velocity increases, the coefficient of friction increases. In this case, when load 10 N and sliding velocity increases, the friction values increases. Gradually, when the friction increases at 1.5 m/sec of sliding velocity and 20 N, the friction between the pin and disc is higher.

TABLE 3: Results of experiments.

| S. no | Graphite % | TiC % | Sliding speed | Load | Sliding velocity | Wear loss | COF |
|---|---|---|---|---|---|---|---|
| 1 | 3 | 5 | 400 | 10 | 0.5 | 0.0041 | 0.241 |
| 2 | 3 | 5 | 400 | 10 | 1 | 0.0051 | 0.253 |
| 3 | 3 | 5 | 400 | 10 | 1.5 | 0.005 | 0.29 |
| 4 | 3 | 10 | 500 | 15 | 0.5 | 0.0049 | 0.232 |
| 5 | 3 | 10 | 500 | 15 | 1 | 0.0049 | 0.25 |
| 6 | 3 | 10 | 500 | 15 | 1.5 | 0.0056 | 0.291 |
| 7 | 3 | 15 | 600 | 20 | 0.5 | 0.0044 | 0.226 |
| 8 | 3 | 15 | 600 | 20 | 1 | 0.0051 | 0.258 |
| 9 | 3 | 15 | 600 | 20 | 1.5 | 0.0066 | 0.286 |
| 10 | 4 | 5 | 500 | 20 | 0.5 | 0.0056 | 0.288 |
| 11 | 4 | 5 | 500 | 20 | 1 | 0.0056 | 0.309 |
| 12 | 4 | 5 | 500 | 20 | 1.5 | 0.006 | 0.317 |
| 13 | 4 | 10 | 600 | 10 | 0.5 | 0.0055 | 0.243 |
| 14 | 4 | 10 | 600 | 10 | 1 | 0.0048 | 0.269 |
| 15 | 4 | 10 | 600 | 10 | 1.5 | 0.0062 | 0.283 |
| 16 | 4 | 15 | 400 | 15 | 0.5 | 0.0048 | 0.215 |
| 17 | 4 | 15 | 400 | 15 | 1 | 0.0054 | 0.233 |
| 18 | 4 | 15 | 400 | 15 | 1.5 | 0.0048 | 0.261 |
| 19 | 5 | 5 | 600 | 15 | 0.5 | 0.0074 | 0.288 |
| 20 | 5 | 5 | 600 | 15 | 1 | 0.0082 | 0.281 |
| 21 | 5 | 5 | 600 | 15 | 1.5 | 0.0089 | 0.313 |
| 22 | 5 | 10 | 400 | 20 | 0.5 | 0.0054 | 0.274 |
| 23 | 5 | 10 | 400 | 20 | 1 | 0.0063 | 0.285 |
| 24 | 5 | 10 | 400 | 20 | 1.5 | 0.0066 | 0.305 |
| 25 | 5 | 15 | 500 | 10 | 0.5 | 0.0045 | 0.222 |
| 26 | 5 | 15 | 500 | 10 | 1 | 0.004 | 0.239 |
| 27 | 5 | 15 | 500 | 10 | 1.5 | 0.006 | 0.271 |



Main Effects Plot for SN ratios
Wear Loss

Signal-to-noise: Smaller is better
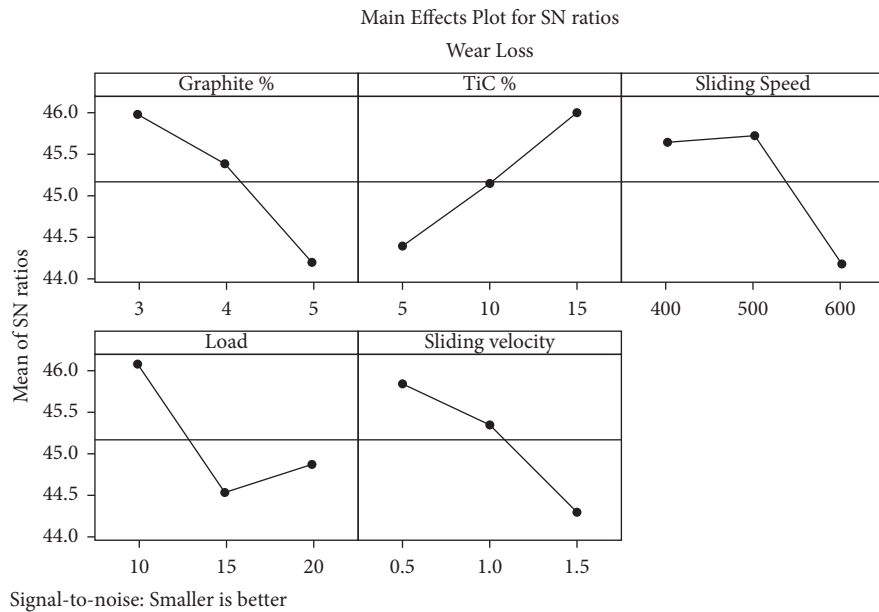
FIGURE 2: S/N ratio for wear loss.

TABLE 4: ANOVA for wear loss.

| Source | DF | Seq SS | Adj SS | Adj MS | F | P |
|---|---|---|---|---|---|---|
| Graphite % | 2 | 0.0000083 | 0.0000083 | 0.0000041 | 16.19 | 0 |
| TiC % | 2 | 0.0000059 | 0.0000059 | 0.000003 | 11.62 | 0.001 |
| Sliding speed | 2 | 0.0000073 | 0.0000073 | 0.0000037 | 14.37 | 0 |
| Load | 2 | 0.0000055 | 0.0000055 | 0.0000027 | 10.75 | 0.001 |
| Sliding velocity | 2 | 0.0000048 | 0.0000048 | 0.0000024 | 9.44 | 0.002 |
| Error | 16 | 0.0000041 | 0.0000041 | 0.0000003 | | |
| Total | 26 | 0.0000359 | | | | |

TABLE 5: ANOVA for COF.

| Source | DF | Seq SS | Adj SS | Adj MS | F | P |
|---|---|---|---|---|---|---|
| Graphite % | 2 | 0.0012998 | 0.0012998 | 0.0006499 | 9.68 | 0.002 |
| TiC % | 2 | 0.0077158 | 0.0077158 | 0.0038579 | 57.44 | 0 |
| Sliding speed | 2 | 0.0004563 | 0.0004563 | 0.0002282 | 3.4 | 0.059 |
| Load | 2 | 0.0034588 | 0.0034588 | 0.0017294 | 25.75 | 0 |
| Sliding velocity | 2 | 0.0084748 | 0.0084748 | 0.0042374 | 63.1 | 0 |
| Error | 16 | 0.0010745 | 0.0010745 | 0.0000672 | | |
| Total | 26 | 0.02248 | | | | |
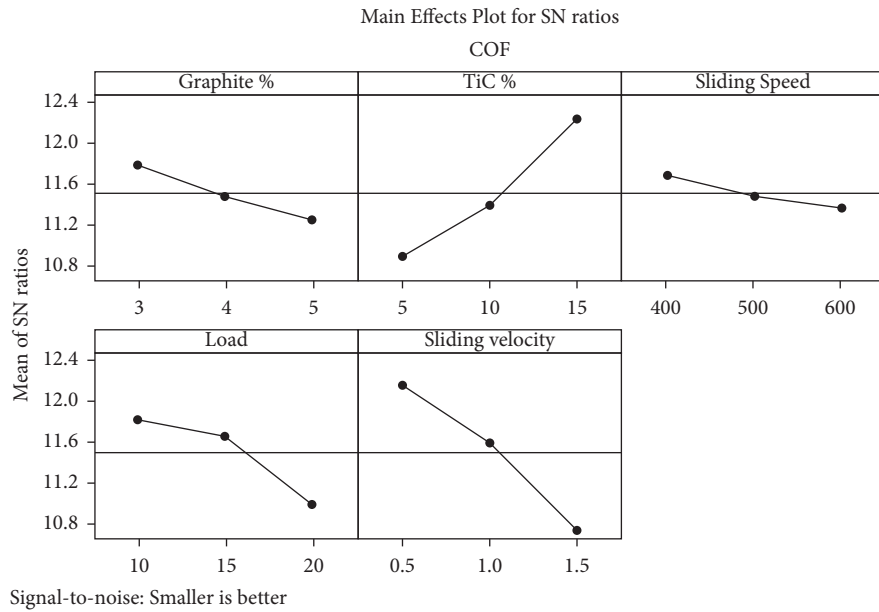


FIGURE 3: S/N ratio for coefficient of friction.
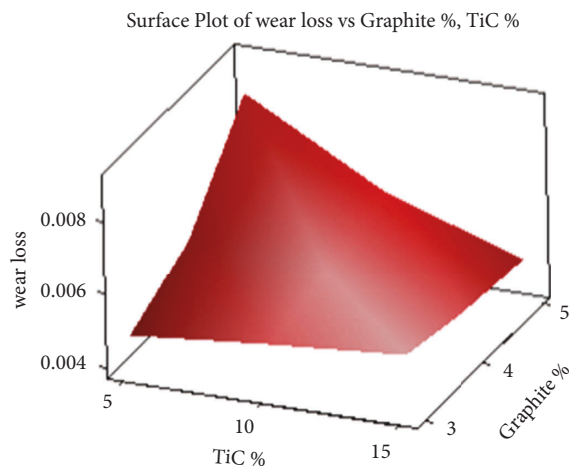


FIGURE 4: Surface plot graph for TiC % VS graphite % to wear loss.
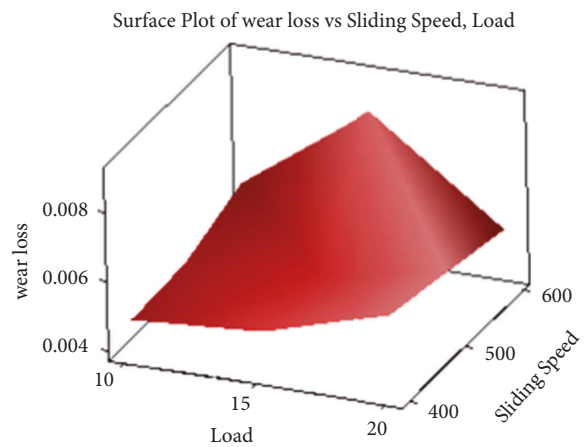


FIGURE 5: Surface plot graph for load % VS sliding speed to wear loss.

## 4. Wornout Analysis

Figure 10 shows the wornout surface of the after wear composites. Figure 10(a) shows the presence of 15% of TiC and 3 % of graphite with the load of 10 N. The wornout surfaces are very low, and this is due to the hardness of the composite. In this case, at that level, the reinforcement particles are strongly bonded with the matrix phase, then the surface is very smooth. Also, it is clearly observed that the 3%
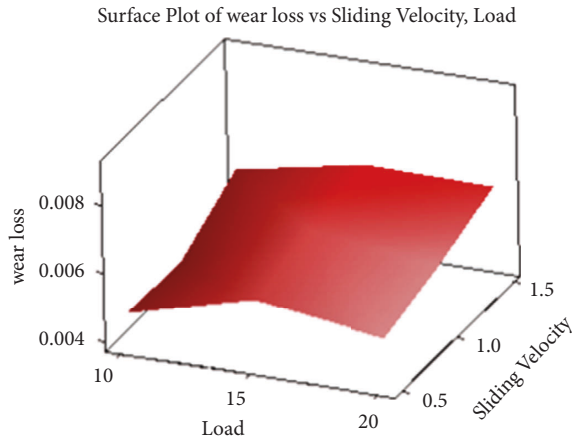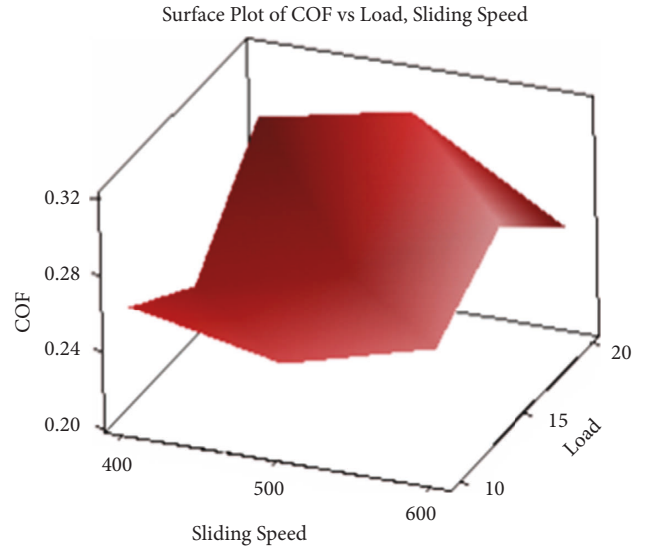
Surface Plot of wear loss vs Sliding Velocity, Load



FIGURE 6: Surface plot graph for load % VS sliding velocity to wear loss.

Surface Plot of COF vs Graphite %, TiC %



FIGURE 7: Surface plot graph for graphite % vs TiC to COF.

Surface Plot of COF vs Load, Sliding Speed



FIGURE 8: Surface plot graph for load % VS sliding speed to COF.

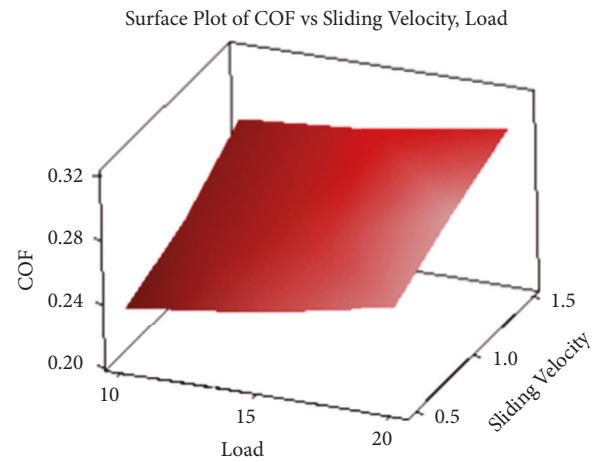Surface Plot of COF vs Sliding Velocity, Load



FIGURE 9: Surface plot graph for load % vs sliding distance to COF.

of graphite have experienced a minimal wear. This is due to the self-lubrication effect of graphite on the tribo surface [25]. Figure 10(b) shows the presence of 10% TiCi and 4% of Graphite with the load capacity of 15 N. In this case, the wornout surface has a mild groove on the surface of the matrix. Due to the increase in load and 2% of graphic particles, the hardness of the composites is low at that level. Figure 10(c) shows the presence of 5% of TiC with 4% of graphite and at 15 N of the applied load, the wear debris is very high. This shows severe plastic flow of material at low

applied loads. At high applied load and high sliding velocity, the flake-like debris is formed as an outcome of delamination of the tribo surface [26]. Figure 10(d) shows the presence of TiC at 5% and 5% of graphite and applied load at 20 N. During the maximum load, the delamination of the reinforcement from the matrix is very high due to the 5% of TiC presence in the material. In the graphite 5% case, the
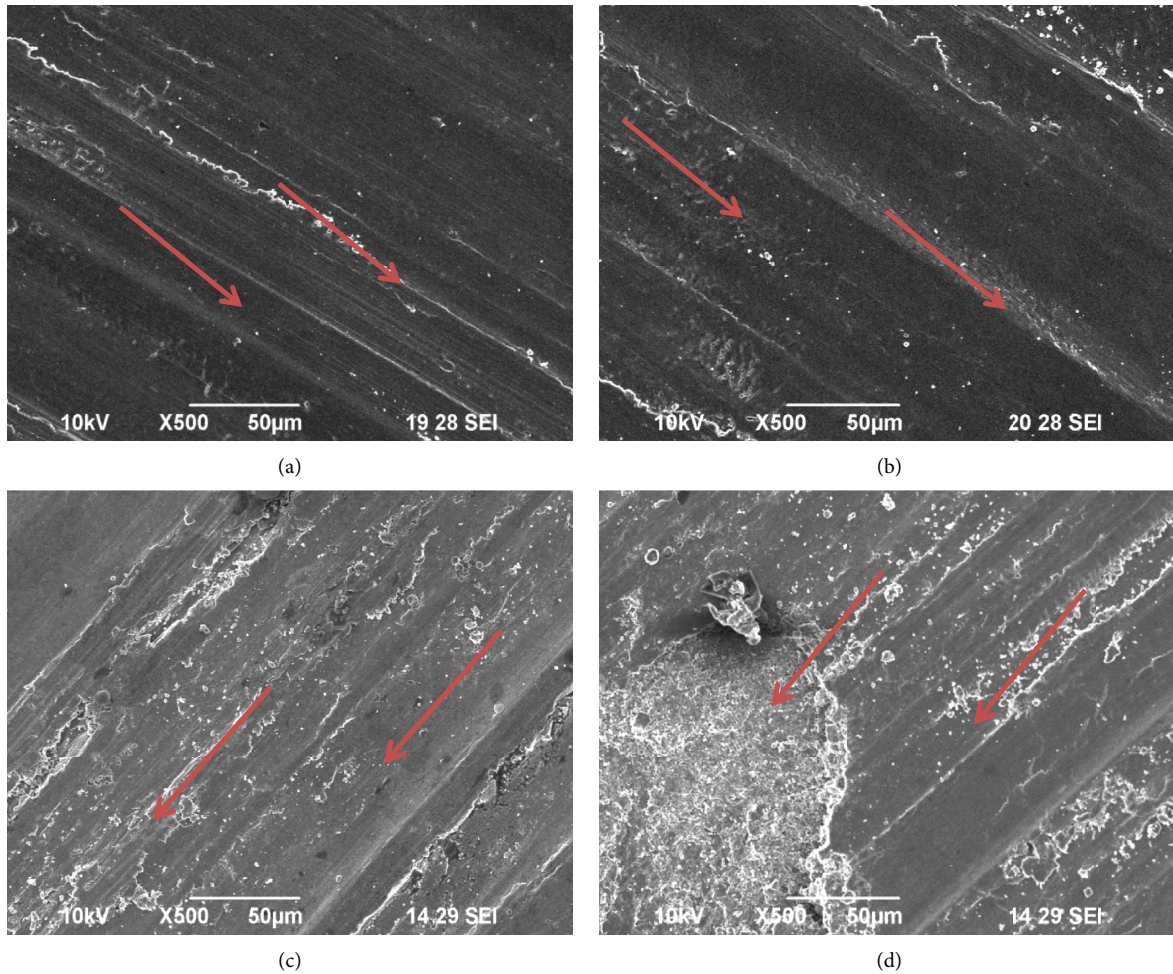
Figure 10: (a) TiC 15%, graphite 3%, and load 10N; (b) TiC 10%, graphite 4%, and load 15N; (c) TiC 5%, graphite 4%, and Load 15N (d). TiC 5%, graphite 45%, and load 20N.

hardness of the composite is very low and also it provides self-lubricant properties which cause slowly decrease and leads to the maximum delamination of the reinforcement.

## 5. Conclusion

(1) Al7075/TiC/Gr was fabricated using the liquid metallurgy process, and Taguchi method was adapted to find the optimum combination of input parameters.

(2) Load and TiC % are the most influencing parameters for wear loss, At 20N of applied load and 15% of TiC, the wear loss decreases. The optimum combination for minimum wear loss is 3% of graphite and 15% of TiC, 10 N of applied load, 400 rpm of sliding distance, and 0.5 m/s of sliding velocity offers minimum wear loss.

(3) Coefficient of friction is minimum when TiC percentage increases. Load is the maximum parameter, which increases the friction between the pin and the disc. The optimum combination for lower coefficient of friction is 3% of graphite and 15% of TiC, 10 N of applied load, 400 rpm of sliding distance, and 0.5 m/s of sliding velocity offers minimum friction in developed Al7075/TiC/ Gr composites.

(4) The wornout images shows the different consequences of various influencing parameters which affects the wear loss and coefficient of friction using SEM images. Through which, it is identified as 15% of TiC and 3% of graphite, which shows minimum delamination and small groove in after wear composites.

## Data Availability

All the associated data are provided in the article.

## Conflicts of Interest

The authors declare that they have no conflicts of interest.

## References

[1] S. Mosleh-Shirazi, F. Akhlaghi, and D. Y. Li, "Effect of SiC content on dry sliding wear, corrosion and corrosive wear of

Al/SiC nanocomposites," *Transactions of Nonferrous Metals Society of China*, vol. 26, no. 7, pp. 1801–1808, 2016.

[2] D. Jeyasimman, R. Narayanasamy, R. Ponalagusamy, V. Anandakrishnan, and M. Kamaraj, "The effects of various reinforcements on dry sliding wear behaviour of AA 6061 nanocomposites," *Materials & Design*, vol. 64, pp. 783–793, 2014.

[3] D. M. Shinde, S. Poria, and P. Sahoo, "Dry sliding wear behavior of ultrasonic stir cast boron carbide reinforced aluminium nanocomposites," *Surface Topography: Metrology and Properties*, vol. 8, no. 2, Article ID 025033, 2020.

[4] T. S. Sachit, N. Mohan, R. Suresh, and M. A. Prasad, "Optimization of dry sliding wear behavior of aluminum LM4-Ta/NbC nano composite using Taguchi technique," *Materials Today Proceedings*, vol. 27, pp. 1977–1983, 2020.

[5] G. Cao, H. Konishi, and X. Li, "Mechanical properties and microstructure of Mg/SiC nanocomposites fabricated by ultrasonic cavitation based nanomanufacturing," *Journal of Manufacturing Science and Engineering*, vol. 130, no. 3, 2008.

[6] K. J. Joshua, S. J. Vijay, and D. P. Selvaraj, "Effect of nano TiO2 particles on microhardness and microstructural behavior of AA7068 metal matrix composites," *Ceramics International*, vol. 44, no. 17, pp. 20774–20781, 2018.

[7] U. K. G. Annigeri Veeresh Kumar, "Method of stir casting of aluminum metal matrix composites: a review," *Materials Today Proceedings*, vol. 4, no. 2, pp. 1140–1146, 2017.

[8] M. P. Reddy, M. Himyan, F. Ubaid et al., "Enhancing thermal and mechanical response of aluminum using nanolength scale TiC ceramic reinforcement," *Ceramics International*, vol. 44, no. 8, pp. 9247–9254, 2018.

[9] V. Khalili, A. Heidarzadeh, S. Moslemi, and L. Fathyunes, "Production of Al6061 matrix composites with ZrO2 ceramic reinforcement using a low-cost stir casting technique: microstructure, mechanical properties, and electrochemical behavior," *Journal of Materials Research and Technology*, vol. 9, no. 6, pp. 15072–15086, 2020.

[10] A. Siddique, Z. Iqbal, Y. Nawab, and K. Shaker, "A review of joining techniques for thermoplastic composite materials," *Journal of Thermoplastic Composite Materials*, Article ID 089270572210966, 2022.

[11] V. R. Rao, N. Ramanaiah, and M. M. M. Sarcar, "Dry sliding wear behavior of Al7075 reinforced with titanium carbide (TiC) particulate composites," in *Proceedings of the International Conference on Advances in Materials, Manufacturing and Applications*, AMMA, NIT,Tiruchirapally, April 2015.

[12] K. Hemadri, S. Ajith Arul Daniel, A. Parthiban, and T. Vinod kumar, "Investigation on the response parameters in electric discharge machining of developed aluminium metal matrix composites," *Materials Today Proceedings*, 2022.

[13] R. Gukendran, M. Sambathkumar, K. S. K. Sasikumar, K. Ponappa, and S. Gopal, "Investigation of dry sliding wear behavior of al 7075–(SiC/TiC) hybrid metal matrix composites," *Surface Review and Letters*, vol. 28, no. 07, Article ID 2150065, 2021.

[14] S. Basavarajappa, G. Chandramohan, K. Mukund, M. Ashwin, and M. Prabu, "Dry sliding wear behavior of Al 2219/SiCp-Gr hybrid metal matrix composites," *Journal of Materials Engineering and Performance*, vol. 15, no. 6, pp. 668–674, 2006.

[15] L. Jinfeng, J. Longtao, W. Gaohui, T. Shoufu, and C. Guoqin, "Effect of graphite particle reinforcement on dry sliding wear of SiC/Gr/Al composites," *Rare Metal Materials and Engineering*, vol. 38, no. 11, pp. 1894–1898, 2009.

[16] S. A. A. Daniel and PM. Gopal, "Study on tribological behaviour of Al/SiC/MoS2 hybrid metal matrix composites in high temperature environmental condition," *Silicon*, vol. 10, no. 5, pp. 2129–2139, 2018.

[17] A. Kumar, V. Kumar, A. Kumar, B. Nahak, and R. Singh, "Investigation of mechanical and tribological performance of marble dust 7075 aluminium alloy composites," *Materials Today Proceedings*, vol. 44, pp. 4542–4547, 2021.

[18] K. Almadhoni and S. Khan, "Review of effective parameters of stir casting process on metallurgical properties of ceramics particulate Al composites," *IOSR Journal of Mechanical and Civil Engineering*, vol. 12, no. 6, pp. 2278–1684, 2015.

[19] A. A. Daniel, S. Murugesan, and S. Sukkasamy, "Dry sliding wear behaviour of aluminium 5059/SiC/MoS 2 hybrid metal matrix composites," *Materials Research*, vol. 20, no. 6, pp. 1697–1706, 2017.

[20] M. Azadi, A. S. Rouhaghdam, S. Ahangarani, and H. H. Mofidi, "Mechanical behavior of TiN/TiC multilayer coatings fabricated by plasma assisted chemical vapor deposition on AISI H13 hot work tool steel," *Surface and Coatings Technology*, vol. 245, pp. 156–166, 2014.

[21] K. Hemadri, S. Ajith Arul Daniel, V. Kukanur, S. Vijayananth, and R. Kumar, "Investigation on mechanical characterization of Al/Mos2/WC hybrid composite," *Materials Today Proceedings*, 2022.

[22] J. Lakshmipathy and B. Kulendran, "Reciprocating wear behavior of 7075Al/SiC in comparison with 6061Al/Al2O3 composites," *International Journal of Refractory Metals and Hard Materials*, vol. 46, pp. 137–144, 2014.

[23] A. Baradeswaran and A. E. Perumal, "Wear and mechanical characteristics of Al 7075/graphite composites," *Composites Part B: Engineering*, vol. 56, pp. 472–476, 2014.

[24] A. Kovalchenko, O. Ajayi, A. Erdemir, G. Fenske, and I. Etsion, "The effect of laser texturing of steel surfaces and speed-load parameters on the transition of lubrication regime from boundary to hydrodynamic," *Tribology Transactions*, vol. 47, no. 2, pp. 299–307, 2004.

[25] L. Wang, G. Zhang, Y. Wang, Y. Wang, X. Sun, and Q. Xue, "TiC/aC: H nanocomposite coatings as substitute for MoS2-based solid lubrication in helium atmosphere," *Journal of Non-Crystalline Solids*, vol. 358, no. 1, pp. 65–71, 2012.

[26] P. Loganathan, A. Gnanavelbabu, and K. Rajkumar, "Analysis and characterization of friction behaviour on AA7075/ZrB2 composite under dry sliding condition," *Materials Research Express*, vol. 6, no. 2, p. 026576, 2018.